Acoustic methods for high-throughput protein crystal mounting at next-generation macromolecular crystallographic beamlines

Christian G. Roessler,[a] Anthony Kuczewski,[a] Richard Stearns,[b] Richard Ellson,[b] Joseph Olechno,[b] Allen M. Orville,[a,c] Marc Allaire,[a] Alexei S. Soares[a]* and Annie Héroux[a]*

[a]Photon Sciences Directorate, Brookhaven National Laboratory, Upton, NY 11973, USA, [b]Labcyte Inc., 1190 Borregas Avenue, Sunnyvale, CA 94089, USA, and [c]Biosciences Department, Brookhaven National Laboratory, Upton, NY 11973, USA. E-mail: soares@bnl.gov, heroux@bnl.gov

To take full advantage of advanced data collection techniques and high beam flux at next-generation macromolecular crystallography beamlines, rapid and reliable methods will be needed to mount and align many samples per second. One approach is to use an acoustic ejector to eject crystal-containing droplets onto a solid X-ray transparent surface, which can then be positioned and rotated for data collection. Proof-of-concept experiments were conducted at the National Synchrotron Light Source on thermolysin crystals acoustically ejected onto a polyimide 'conveyor belt'. Small wedges of data were collected on each crystal, and a complete dataset was assembled from a well diffracting subset of these crystals. Future developments and implementation will focus on achieving ejection and translation of single droplets at a rate of over one hundred per second.

1. Introduction

Sample mounting automation has become standard at most new macromolecular crystallographic (MX) beamlines and has enabled remote data collection programs to flourish. Currently, most MX automounting systems fall into two categories: pneumatic automounters (Snell et al., 2004) and multi-axis articulated robotic arms systems. Both systems extract crystals which have been mounted on a metallic base from a cryogenic storage Dewar, then place the bases on a magnetic goniometer head for data collection. The time to complete one cycle of sample replacement using these systems is several tens of seconds at best, and significantly longer when bases need to be warmed and dried prior to returning to the storage Dewar. Given that other steps in the data collection process, such as sample centering, data collection strategy decisions and data acquisition, currently impose greater time demands, there has been little need to further decrease automounter duty cycle rates. However, advances in pixel array detectors, data analysis pipelines and the availability of higher flux storage rings have significantly reduced the time to collect diffraction datasets. As such, it is expected that the sample mounting step will soon provide the greatest bottleneck in sample throughput.

Several systems have been proposed to address this bottleneck. In situ plate screening allows data collection on samples sitting in their originating solution (Kisselman et al., 2011; le Maire et al., 2011; Soliman et al., 2011), provided that individual crystals can be resolved. Microfluidic devices can flow crystal-containing solutions through sealed channels and passage them in the beam (Yadav et al., 2005; Gerdts et al., 2006, 2008; Hansen et al., 2006; Li et al., 2006; Ng et al., 2008; Emamzadah et al., 2009). Both methods share similar drawbacks in that they are only compatible with room-temperature data collection and they encapsulate the samples in containers that impose restricted geometries for data collection. Ultimately, to keep pace with the sub-second data collection rates proposed for next-generation MX beamlines, ex situ methods will be needed to house and quickly transfer samples into the X-ray beam.

A new crystal transfer method uses acoustic droplet ejection (ADE) technology to eject crystal-containing droplets out of a sample well and onto a solid destination surface. ADE uses short tone bursts of acoustic energy focused at the surface of a liquid reservoir to eject discrete droplets with high positional precision and repeatability (Elrod et al., 1989). Demonstrated applications for MX include transferring microcrystals for seeding (Villaseñor et al., 2010) and populating sample meshes on pins for data collection (Soares et al., 2011). Previously, ADE methods were incompatible with the geometric constraints and goniometric hardware in place at most MX beamlines. To make this capability available at a beamline, we constructed an ADE system to place crystal-containing droplets onto an X-ray transparent 'conveyor belt', position the crystals in the X-ray beam and acquire diffraction data on cryo-cooled samples. Implications for high-throughput data collection, in particular for microcrystals and X-ray radiation-sensitive samples, will be discussed.

short communications

2. Materials and methods

Reagents and thermolysin were purchased from Sigma-Aldrich (St Louis, Missouri, USA) and used without further purification. Crystallization of hexagonal thermolysin was performed as previously described (Marshall *et al.*, 2012), with the modification that 5–15% (*w/v*) ethylene glycol was added to the crystallization conditions. After two days, crystal-containing droplets were pooled, the concentration of ethylene glycol was adjusted to 30% (*w/v*), and the sample was briefly centrifuged at $1000 \times g$. Most of the mother liquor was aspirated and the crystals were gently re-suspended to form a slurry where approximately half of the sample volume consisted of crystalline protein.

An ADE system, similar in construction to what has been reported (Aerni *et al.*, 2005), was installed at beamline X25 at the National Synchrotron Light Source (NSLS). Central to this system was a 10 MHz spherically focused transducer (GE Inspection Technologies LP, Lewistown, Pennsylvania, USA) which, when excited by a 550 µs radiofrequency burst at peak frequency for a total of 20 mW RMS power, produced 3–10 nl droplets per burst.

A motorized conveyor belt apparatus was designed to be compact and compatible with standard MX beamline configurations. Consequently, a standard goniometer head was replaced by a conveyor belt which consisted of two rollers, one of which was driven by a compact stepper motor (Faulhaber, Germany) of the type used to drive κ rotation on the X25 goniometer (Fig. 1). This motor was controlled under EPICS through the data acquisition software (Skinner & Sweet, 1998; Skinner *et al.*, 2006). A custom-fit strip of Kapton polyimide tape (DuPont, Wilmington, Delaware, USA), about 4 mm in width and 30 cm long, was stretched between the rollers. The entire conveyor belt assembly is approximately 20 cm long and 5 cm wide.

Twenty microliters of thermolysin crystal slurry was loaded into a well of an acoustically compatible microplate (Labcyte Inc., Sunnyvale, California, USA). The microplate was positioned with well openings facing upwards underneath the conveyor belt, and the transducer was aligned directly beneath the sample well. The microplate position was controlled by a motorized *XYZ* translation stage independent of the transducer stage, which enabled accurate alignment of both the microplate and the transducer to each other and the conveyor belt. Individual droplets were acoustically ejected
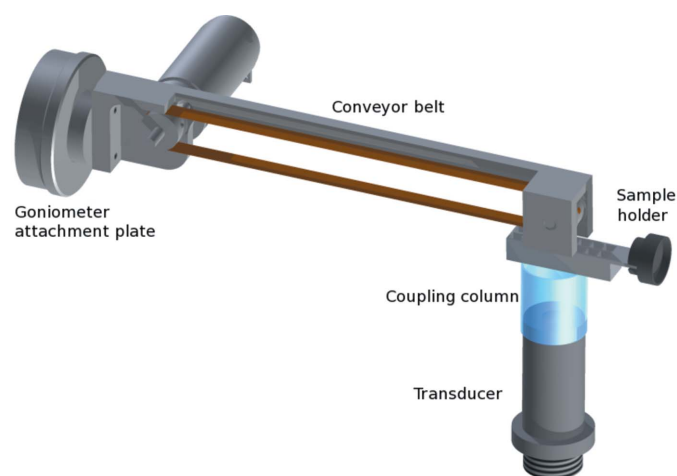

Figure 1
Computer design of an ADE ejector and conveyor belt. A motorized two-roller conveyor belt apparatus attaches to a goniometer *via* an attachment plate. A 16-well magnetic base-mounted sample holder and transducer sit below the conveyor belt. A coupling tube containing water couples the transducer to the underside of the sample holder.

and deposited onto the conveyor belt, then immediately translated into position at a rate of approximately 1 cm s^{-1} for cryo-cooling at 100 K using a Cryostream 700 (Oxford Cryosystems, Oxford, UK). Crystals were located in each droplet with an automated X-ray raster scan using a 100 µm × 100 µm beam size, exposing for 0.5 s with a 0.5° oscillation per step. Typical rastering times for a 1 mm × 1 mm droplet was 2 min. Datasets of up to 30° of rotation were collected with negligible vibration on the Kapton tape by the Cryostream. A data collection strategy was employed that used an oscillation of 0.5° s^{-1} at λ = 1.1 Å. Datasets were indexed, integrated and individually scaled using *iMOSFLM* (Battye *et al.*, 2011). Manual inspection revealed three datasets with good statistics and resolutions better than 1.9 Å. These datasets were re-indexed and scaled together using *POINTLESS* and *AIMLESS* (Evans, 2006).

3. Results and discussion

Nanoliter-volume droplets of a thermolysin crystal slurry were deposited onto a conveyor belt using an acoustic ejector and translated into a cryogenic gas stream. Ejections were successful for several types of slurries, including those composed of larger (100–200 µm-diameter) crystals, and solutions containing smaller crystals (20–80 µm). Crystal size was controlled by changing the concentration of ethylene glycol in the precipitant solution, producing larger crystals with 15% (*w/v*) and smaller crystals with 5% (*w/v*). The larger sized crystals tended to settle to the bottom of the well during acoustic transfer. Consequently, approximately one-third of the drops contained a single crystal, as judged by the presence of reflections with $I/\sigma I > 5$. For the latter type of samples, every drop contained at least one crystal, and often contained as many as ten individual crystals.

The conveyor belt system is optimized for high-throughput data collection on high-flux sources. Given that the average crystal lifetime in an un-attenuated beam at next-generation MX beamlines is projected to be in the microsecond range (*e.g.* Schneider *et al.*, 2013), it becomes more feasible to collect small wedges of data from multiple samples in order to construct a full dataset. This also has the benefit of spreading the X-ray dose among many samples, reducing radiation-induced structural changes. To simulate this strategy of data acquisition we collected small wedges (total oscillation $\leq$ 30°) of diffraction data on 22 crystals within 12 droplets. Manual inspection identified three well diffracting partial datasets which, when merged together, produced a single dataset with high completeness (Table 1). It is notable that the data quality (resolution, mosaicity, *etc.*) for each thermolysin crystal varied randomly, even for samples within the same droplet (see Table S1 of supplementary material[1]).

We intentionally designed the conveyor belt to be compatible with a standard MX goniometer set-up. First, it simplifies the transition between the standard and ADE modes of data collection at the beamline. Second, re-purposing already defined motors makes it simple to create complex motions for alignment while using the same data-collection GUI. For example, cryo-cooling of the droplets without forming ice succeeded only after defining a fast rotation/translation of the belt from the eject position (with the belt perpendicular to the cold flow) to the collect position (parallel to the cold stream) (Fig. 2 and supplementary movie 1). With our optimized command stream, all of these actions are coordinated through standard beamline software and occur within a matter of seconds.

Table 1
Processing and refinement statistics for diffraction data from acoustically injected thermolysin crystals.

Values in parentheses are for the highest-resolution shell. Data are merged from datasets obtained from three different crystals.

Processing	
Resolution (Å)	46.42–1.75 (1.78–1.75)
Measured reflections	204852
Unique reflections	3347
Multiplicity	6.1 (2.3)
R_{merge} (%)†	26.7 (45.1)
R_{meas} (%)‡	28.6 (56.9)
$CC_{1/2}$§	0.975 (0.755)
Completeness (%)	98.7 (90.8)
Mean $I/\sigma I$	6.2 (2.0)
Refinement (PDB entry 4tln)	
R_{work}/R_{free} (%)	14.3/18.2
Total atoms included	2926
Water atoms included	446
R.m.s.d. bond length (Å)	2.05
R.m.s.d. bond angle (°)	1.90

† $R_{merge} = \Sigma_{hkl}\Sigma_i|I_i(hkl) - \langle I(hkl)\rangle|/\Sigma_{hkl}\Sigma_iI_i(hkl)$, where $I(hkl)$ is the intensity of reflection hkl, Σ_{hkl} is the sum over all reflections and Σ_i is the sum over i measurements of reflection hkl. ‡ $R_{meas} = \Sigma_{hkl}[N/(N-1)]^{1/2}\Sigma_i|I_i(hkl) - \langle I(hkl)\rangle|/\Sigma_{hkl}\Sigma_iI_i(hkl)$, where hkl is a particular reflection, N is the multiplicity of reflection hkl, $I_i(hkl)$ is the ith intensity measurement of reflection hkl and $\langle I(hkl)\rangle$ is the average intensity of reflection hkl. § $CC_{1/2}$ is calculated by splitting the data randomly in half (Diederichs & Karplus, 2013).

A new paradigm for MX data measurements is emerging, due mostly to next-generation synchrotrons and X-ray free-electron lasers. Samples which are not amenable to traditional data collection experiments due to their small size, radiation sensitivity or chemical composition are proving more suitable for high-flux micro-focus beamline data collection (Sanishvili *et al.*, 2011). Subsequently, the time each sample spends in the beam is decreasing while the number of samples needed to generate a full dataset is increasing. New systems dealing with increased sample throughput are already needed to alleviate the bottleneck in data collection at MX beamlines. ADE onto solid supports addresses this problem by reducing the time to bring a new droplet into the X-ray beam to a few milliseconds. Further developments are now required to increase the speed of crystal location and centering on the conveyor belt.

With an ADE system integrated into an endstation, collecting highly redundant datasets while minimizing radiation dose effects opens the possibility for routine phasing from native sulfur anomalous signals (Liu *et al.*, 2012). There are also several examples of radiation-damage-prone systems, particularly in the class of metalloenzymes, which would benefit from limited X-ray exposure per crystal (Daughtry *et al.*, 2012). Finally, the ability to screen for ligand binding to a protein target would be greatly aided by faster sample throughput methods (Allaire *et al.*, 2009). Since only nanoliter volumes are transferred per ejection, preparation of several microliters of sample allows for thousands of droplets to be deposited, mixed with a sample from a chemical library or cryogenic agent, and soaked briefly on the conveyor belt before freezing for data collection. Given our initial results using ADE technology in combination with a conveyor belt system, there is hope that cryo-cooled data collections will take full advantage of high-flux MX beamlines at new synchrotron sources.

Data for this study were measured at beamline X25 of the National Synchrotron Light Source (NSLS). This work was supported by the Brookhaven National Laboratory/US Department of Energy, Laboratory Directed Research and Development grant 11-008, from the DOE Office of Biological and Environmental Research (FWP

(a)

(b)

Figure 2
ADE ejector and conveyor belt testing at X25 at NSLS. (a) Ejection position. The conveyor belt is positioned directly over the sample well, outside of the Cryostream gas stream, ready to receive a droplet on the underside of the Kapton belt. (b) Collect position. Following droplet ejection, the conveyor belt is translated up, rotated 90°, and the belt is translated so that the droplet is in the cold gas stream and beam path.

References

Aerni, H.-R., Cornett, D. S. & Caprioli, R. M. (2005). *Anal. Chem.* **78**, 827–834.

Allaire, M., Moiseeva, N., Botez, C. E., Engel, M. A. & Stephens, P. W. (2009). *Acta Cryst.* **D65**, 379–382.

Battye, T. G. G., Kontogiannis, L., Johnson, O., Powell, H. R. & Leslie, A. G. W. (2011). *Acta Cryst.* **D67**, 271–281.

Daughtry, K. D., Xiao, Y., Stoner-Ma, D., Cho, E., Orville, A. M., Liu, P. & Allen, K. N. (2012). *J. Am. Chem. Soc.* **134**, 2823–2834.

Diederichs, K. & Karplus, P. A. (2013). *Acta Cryst.* **D69**, 1215–1222.

Elrod, S. A., Hadimioglu, B., Khuri, x, Yakub, B. T., Rawson, E. G., Richley, E., Quate, C. F., Mansour, N. N. & Lundgren, T. S. (1989). *J. Appl. Phys.* **65**, 3441–3447.

Emamzadah, S., Petty, T. J., De Almeida, V., Nishimura, T., Joly, J., Ferrer, J.-L. & Halazonetis, T. D. (2009). *Acta Cryst.* **D65**, 913–920.

Evans, P. (2006). *Acta Cryst.* D**62**, 72–82.

Gerdts, C. J., Elliott, M., Lovell, S., Mixon, M. B., Napuli, A. J., Staker, B. L., Nollert, P. & Stewart, L. (2008). *Acta Cryst.* D**64**, 1116–1122.

Gerdts, C. J., Tereshko, V., Yadav, M. K., Dementieva, I., Collart, F., Joachimiak, A., Stevens, R. C., Kuhn, P., Kossiakoff, A. & Ismagilov, R. F. (2006). *Angew. Chem. Int. Ed.* **45**, 8156–8160.

Hansen, C. L., Classen, S., Berger, J. M. & Quake, S. R. (2006). *J. Am. Chem. Soc.* **128**, 3142–3143.

Kisselman, G., Qiu, W., Romanov, V., Thompson, C. M., Lam, R., Battaile, K. P., Pai, E. F. & Chirgadze, N. Y. (2011). *Acta Cryst.* D**67**, 533–539.

Li, L., Mustafi, D., Fu, Q., Tereshko, V., Chen, D. L., Tice, J. D. & Ismagilov, R. F. (2006). *Proc. Natl Acad. Sci.* **103**, 19243–19248.

Liu, Q., Dahmane, T., Zhang, Z., Assur, Z., Brasch, J., Shapiro, L., Mancia, F. & Hendrickson, W. A. (2012). *Science*, **336**, 1033–1037.

Maire, A. le, Gelin, M., Pochet, S., Hoh, F., Pirocchi, M., Guichou, J.-F., Ferrer, J.-L. & Labesse, G. (2011). *Acta Cryst.* D**67**, 747–755.

Marshall, H., Venkat, M., Hti Lar Seng, N. S., Cahn, J. & Juers, D. H. (2012). *Acta Cryst.* D**68**, 69–81.

Ng, J. D., Clark, P. J., Stevens, R. C. & Kuhn, P. (2008). *Acta Cryst.* D**64**, 189–197.

Sanishvili, R., Yoder, D. W., Pothineni, S. B., Rosenbaum, G., Xu, S., Vogt, S., Stepanov, S., Makarov, O. A., Corcoran, S., Benn, R., Nagarajan, V., Smith, J. L. & Fischetti, R. F. (2011). *Proc. Natl Acad. Sci.* **108**, 6127–6132.

Schneider, D. K., Berman, L. E., Chubar, O., Hendrickson, W. A., Hulbert, S. L., Lucas, M., Sweet, R. M. & Yang, L. (2013). *J. Phys. Conf. Ser.* **425**, 012003.

Skinner, J. M., Cowan, M., Buono, R., Nolan, W., Bosshard, H., Robinson, H. H., Héroux, A., Soares, A. S., Schneider, D. K. & Sweet, R. M. (2006). *Acta Cryst.* D**62**, 1340–1347.

Skinner, J. M. & Sweet, R. M. (1998). *Acta Cryst.* D**54**, 718–725.

Snell, G., Cork, C., Nordmeyer, R., Cornell, E., Meigs, G., Yegian, D., Jaklevic, J., Jin, J., Stevens, R. C. & Earnest, T. (2004). *Structure*, **12**, 537–545.

Soares, A. S., Engel, M. A., Stearns, R., Datwani, S., Olechno, J., Ellson, R., Skinner, J. M., Allaire, M. & Orville, A. M. (2011). *Biochemistry*, **50**, 4399–4401.

Soliman, A. S. M., Warkentin, M., Apker, B. & Thorne, R. E. (2011). *Acta Cryst.* D**67**, 646–656.

Villaseñor, A. G., Wong, A., Shao, A., Garg, A., Kuglstatter, A. & Harris, S. F. (2010). *Acta Cryst.* D**66**, 568–576.

Yadav, M. K., Gerdts, C. J., Sanishvili, R., Smith, W. W., Roach, L. S., Ismagilov, R. F., Kuhn, P. & Stevens, R. C. (2005). *J. Appl. Cryst.* **38**, 900–905.